

UNCLASSIFIED

SECURITY CLASSIFICATION OF THIS PAGE (When Data Entered)

REPORT DOCUMENTATION PAGE		READ INSTRUCTIONS BEFORE COMPLETING FORM
1. REPORT NUMBER HDL-TM-79-21	2. GOVT ACCESSION NO.	3. RECIPIENT'S CATALOG NUMBER
4. TITLE (and Subtitle) A Fluidic Approach to the Design of a Mud Pulser for Bore-Hole Telemetry While Drilling		5. TYPE OF REPORT & PERIOD COVERED Technical Memorandum
7. AUTHOR(s) Allen B. Holmes Stacy E. Gehman		6. PERFORMING ORG. REPORT NUMBER
9. PERFORMING ORGANIZATION NAME AND ADDRESS Harry Diamond Laboratories 2800 Powder Mill Road Adelphi, MD 20783		8. CONTRACT OR GRANT NUMBER(s)
11. CONTROLLING OFFICE NAME AND ADDRESS Department of the Interior U.S. Geological Survey Washington, DC 20242		10. PROGRAM ELEMENT, PROJECT, TASK AREA & WORK UNIT NUMBERS
14. MONITORING AGENCY NAME & ADDRESS (if different from Controlling Office)		12. REPORT DATE August 1979
		13. NUMBER OF PAGES 37
		15. SECURITY CLASS. (of this report) UNCLASSIFIED
		15a. DECLASSIFICATION/DOWNGRADING SCHEDULE
16. DISTRIBUTION STATEMENT (of this Report)  Approved for public release; distribution unlimited.		
17. DISTRIBUTION STATEMENT (of the abstract entered in Block 20, if different from Report)		
18. SUPPLEMENTARY NOTES DRCMS Code: 7-36AA-7100 HDL Project: A54735 This research is sponsored by the U.S. Geological Survey, Research and Development Program for OCS Oil and Gas Operations, under Technology Transfer Authorization.		
19. KEY WORDS (Continue on reverse side if necessary and identify by block number) Fluidics Mud pulser Down-hole telemetry Measurement while drilling		
20. ABSTRACT (Continue on reverse side if necessary and identify by block number) Mud-pulse telemetry is a method for communicating diagnostic information from the bottom of a well to the surface while the well is being drilled. Because mud-pulse telemetry offers poten- tial for improving the safety of hazardous offshore drilling oper- ations, the U.S. Geological Survey has sponsored a research program at the Harry Diamond Laboratories (HDL) to investigate the		

DD FORM 1 JAN 73 1473

EDITION OF 1 NOV 65 IS OBSOLETE

UNCLASSIFIED

1

SECURITY CLASSIFICATION OF THIS PAGE (When Data Entered)

UNCLASSIFIED

SECURITY CLASSIFICATION OF THIS PAGE(When Data Entered)

20. Abstract (Cont'd)

feasibility of applying fluidic flow control techniques to the design of a reliable high-speed pulser valve.

During these investigations, three subscale fluidic mud-pulsing circuits were tested over a wide range of drilling-fluid weights and viscosities to simulate well-bore conditions. The tests demonstrated that the unusual rheological properties of drilling mud cause only slight changes in circuit performance. Calculations of dynamic conditions in the drill string indicate that similar full-scale circuits would generate signal pressures of at least 37 psi (255 kPa) at a 200 gal/min (0.76 m<sup>3</sup>/min) circulation rate.

Further tests of circuit dynamic response indicate that a similar full-scale pulser will have a frequency response of 15 to 20 Hz. Analytical investigations have shown that both signal amplitude and frequency response of these test circuits may be improved through design modifications.

HDL is now engaged in an ongoing effort to optimize the geometry of the subscale pulser circuit. A full-scale pulser will then be constructed and tested under surface and downhole conditions so that predicted performance can be verified.

UNCLASSIFIED

SECURITY CLASSIFICATION OF THIS PAGE(When Data Entered)

## 1. INTRODUCTION

Mud-pulse telemetry is a method for transmitting diagnostic information from the bottom of a well to the surface during normal drilling operations. This method has been under development for many years by the drilling industry because of the potentially great improvement that real-time downhole information can provide in drilling efficiency and safety. However, technological problems in pulser design have caused many delays in the application of the concept.

In a mud-pulse telemetry system, electrical signals from sensors near the drill bit are used to actuate a pulser valve. The valve responds by changing its effective port area, which in turn restricts the flow passing through the valve. Each time flow is restricted, a wave of increased pressure is produced through an effect commonly referred to as water hammer. The pressure waves travel through the mud column to the surface where they are detected by a pressure transducer. The sequence of waves is then decoded at the surface and displayed as measurements of downhole parameters for the driller.

Although this method is basically very simple and adaptable for use with conventional drill pipe hardware, the principal factor that has limited its use in the field is the availability of a reliable, high-speed pulser valve.

A mud-pulser valve must operate in severe well-bore environments of pressure, vibration, and shock. A valve of this type must also be designed to handle erosive fluids at flow rates comparable to full circulating rates. The harsh operating environments and physical loads on the valves severely limit the speed and reliability of the mechanical components in mud-pulser valves.

Because mud-pulse telemetry offers great potential for improved safety in offshore drilling operations, the Branch of Marine Oil and Gas Operations of the U.S. Geological Survey (USGS) has funded the U.S. Army's Harry Diamond Laboratories (HDL) to investigate the application of fluidic technology to mud-pulser valve design. Fluidic technology involves the use of fluid flow phenomena to perform control functions such as pressure amplification, digital logic, and flow throttling without moving parts. To perform these functions, fluidics uses only the energy contained in moving fluids and the interaction between these fluids and channels of fixed geometry. As an alternative to mechanical valving, fluidics allows higher operating speeds and increases reliability through the elimination of moving parts and seals.

The specific objectives of the fluidic mud-pulser program reported here were to

(a) determine changes in performance of fluidic components due to the unusual rheological properties of drilling muds,

(b) design fluidic circuits for pulsing mud flows,

(c) measure the performance of subscale circuits with drilling muds as test fluids,

(d) analyze circuit performance data to obtain guidelines for full-scale circuit design, and

(e) calculate dynamic conditions in the drill string so that performance of a full-scale pulser under downhole conditions can be predicted.

## 2. FLUIDIC PULSERS

### 2.1 General

Two fluidic components, a fluidic amplifier and a vortex valve, are employed in the mud-pulser valves described in this report. The components are used to control flow direction and rate in the valve. The essential features of each component are described in the following sections.

### 2.2 Fluidic Amplifier

A general proportional fluidic amplifier configuration is shown in figure 1. Typically, these devices contain a supply jet, one or more control jets, an interaction region, and one or more outlet ports. The channels are rectangular and usually formed by standard milling, chemical etching, or stamping.

Fluid passes through the supply nozzle in the form of a jet flow. Pressure recovered from the jet is available at the output. Control signals, consisting of pressures and flows smaller than those of the supply jet, impinge on the supply jet in the interaction region and deflect the supply jet between two outlets. This, in turn, alters the distribution of pressure across the outputs. Amplification occurs inasmuch as a change in output power in a particular outlet can be achieved with smaller changes in control power. The output may be proportional to the input signals (analog amplifiers, fig. 1) or respond bistably (digital amplifiers) to input commands.

### 2.3 Vortex Valve

The general arrangement of a vortex valve is shown in figure 3. The valve contains two inlet ports, an outlet port--referred to as a sink--and a cylindrical chamber. The sink nozzle has two effective outlet areas which are dependent upon which inlet is pressurized. When the radial inlet is pressurized, flow enters the chamber and travels directly to the sink, undergoing only the small pressure drop associated with entering a reservoir. The effective flow area of the sink is at its maximum value under this condition. When flow enters the chamber through the tangential inlet, a tangential velocity component is imparted to the flow by the chamber walls, and a large pressure drop is developed across the valve because of the centrifugal forces exerted by the rotating fluid. The increased resistance or reduction in effective area reduces the amount of flow which can pass through the valve.

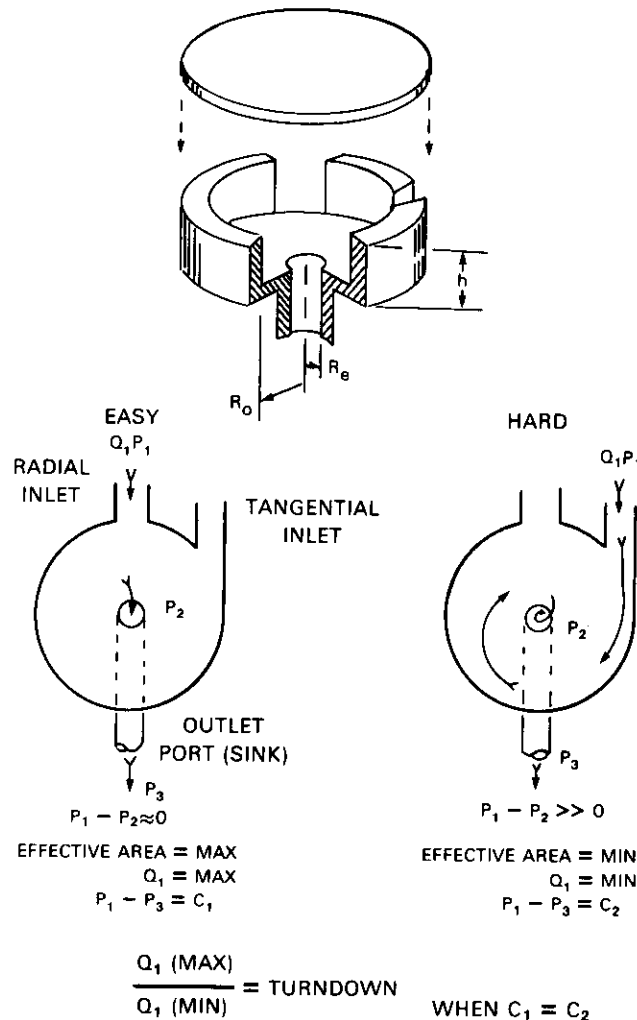


Figure 3. Vortex valve operation showing easy and hard flow directions.

With a constant pressure drop across the valve, the ratio between the maximum flow and minimum flow which can be passed through the valve in each case is used to define the change in effective port area. This ratio, referred to as turndown, is used to indicate the valving effectiveness of the device. In this report the turndown ratio is obtained from measurements of each flow rate at equal pressures between the inlet ports and the pressure at the sink nozzle exhaust. The geometric parameters which influence turndown include normalized radius,  $r_o/r_e$ , and normalized depth,  $h/r_e$ , where  $r_o$  is chamber radius,  $r_e$  is exhaust nozzle radius, and  $h$  is chamber depth.

A great deal of research and development work has been devoted to the study of vortex devices of various types. Results of many of these studies are summarized elsewhere.<sup>2-4</sup> Much of this work was directed towards optimizing turndown and frequency response. Turndown ratios of 3 to 10 are considered typical. Since the effective port area of a given device determines flow capacity and other physical dimensions, it also determines response time.

The response time of a vortex valve is the time required for the effective area or flow through the valve to change from a maximum to a minimum level. Response time has been shown by various experimenters to be proportional to the volume of the vortex chamber and inversely proportional to the flowrate.

#### 2.4 Pulser Circuits

Three pulser circuits were designed and tested during the course of the mud-pulser investigations. Each circuit uses a fluidic amplifier and a vortex valve to produce effective flow area changes. Each circuit is described in terms of its operation as a mud pulser.

---

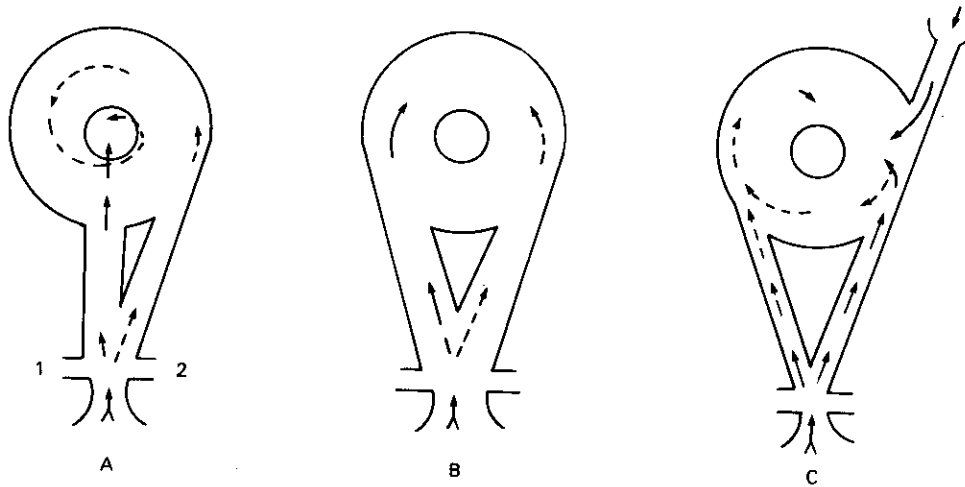
<sup>2</sup>B. E. A. Jacobs and P. J. Baker, *The Steady-State and Transient Performance of Some Large Scale Vortex Diodes*, British Hydromechanics Research Association, Proceedings of the 5th Cranfield Fluidics Symposium, Vol. 1, Uppsala, Sweden (1972).

<sup>3</sup>D. N. Wormley, *A Review of Vortex Diode and Triode Static Characteristics and Dynamic Design Characteristics*, MIT Proceedings of Fluidic State-of-the-Art Symposium, Washington, D.C. (1974).

<sup>4</sup>S. S. Fineblum, *Vortex Diodes*, Bell Laboratories Proceedings, Fluidic State-of-the-Art Symposium, Vol 1, Harry Diamond Laboratories (1974).

## 2.5 Circuit A

Figure 4A describes the essential operating features and general flow configuration of circuit A. In figure 4A the amplifier jet is shown attached to the wall leading to the radial inlet of the vortex valve (solid arrows). Since the flow passes directly to the sink, the resulting pressure drop across the circuit is low. To switch the pulser from this easy-flow state to one in which the flow rate is reduced (the hard-flow state), a control signal in the form of a short-duration pressure pulse is introduced through control port 1.



NOT TO SCALE

Figure 4. Pulser geometries for circuits A, B, and C.

As the control pulse exits the control nozzle, the energy (pressure times flow) in the pulse raises the pressure between the supply jet and the wall. The rise in pressure separates the attached flow from the wall and causes the jet to attach to the opposite wall, as shown by the broken arrows. The energy associated with the supply jet flow produces a vortex which reduces the effective area of the sink nozzle. As the flow area is reduced, the pressure in the radial port increases and reduces the amount of flow which can pass through the amplifier and drill string. The energy of the inlet flow is then expended in compressing the flow entering the valve. A wave (water hammer) of increased pressure forms and propagates back through the string. The pressure is returned to its original level when the jet is deflected by a second control pulse (through port 2) back to its former state. The change in pressure produced by the change in effective flow area or inlet velocity represents the signal which would carry digitized information to the surface.

## 2.6 Circuit B

The operation of circuit B (fig. 4B) is similar to that of circuit A with one exception: the amplifier supply jet is used to alternately pressurize one of two tangential inlets to the vortex chamber. In either stable state, the flow through the pulser is restricted. However, the direction of the rotating flow is reversed each time a signal is applied across the controls. Since the flow rate or pressure drop in the vortex chamber depends on the tangential velocity of rotation and since the tangential velocity goes from a maximum value in one direction through zero to a maximum value in the opposite direction, the flow and pressure in the chamber will vary accordingly. Therefore, during switching there is a momentary increase in flow rate (and effective area) for the pulser. In this circuit the duration of this action--or the length of the pulse which is propagated back through the inlet--is determined by the time required to reverse the flow direction.

## 2.7 Circuit C

Circuit C (fig. 4C) was configured to reduce the physical size of the fluidic amplifier, reduce the nominal energy losses in the amplifier, and reduce the control-signal energy requirements. In this circuit the amplifier passes 50 percent of the total circuit flow; the second tangential inlet carries the remaining 50 percent. The combined effect of the two tangential inlets produces the vortical motion which impedes the flow. However, when the flow is diverted and combines with the flow issuing through the second inlet, the vortex ceases, and the valve discharges flow easily. The flow remains in this condition until a control pulse is applied, and the action is reversed.

## 2.8 Mud-Pulser Circuit Analysis

The performance of a fluidic mud pulser has been analyzed in terms of the flow and pressure conditions in the pulser. This analysis allows for both greater understanding of the loss mechanisms in the pulser and easy comparison of the performance of various pulser models. Losses in the pulser are especially detrimental in the easy flow direction because they not only tend to decrease the turndown ratio but also require a larger pulser to pass the required flow at a given pressure drop.

Losses in a pulser result from loss of dynamic head through friction. These losses occur between the power jet of the fluidic amplifier and the exit nozzle of the vortex valve. The average power jet velocity ( $V_{pj}$ ) is found from the flow rate ( $Q$ ) through the pulser.



$$v_{pj} = \frac{Q}{A_1} \quad , \quad (1)$$

where  $A_1$  is the area of the power jet.

The velocity head of the power jet is the pressure drop from the total pressure ( $P_o$ ) feeding the amplifier to the static pressure ( $P_i$ ) in the amplifier. Thus

$$P_o - P_i = \frac{1}{2} \rho \left( \frac{v_{pj}}{k_1} \right)^2 \quad , \quad (2)$$

where  $\rho$  is the density of the fluid passing through the pulser, and  $k_1$  is the discharge coefficient. A portion of this kinetic energy is lost to turbulence and friction while the fluid passes through the amplifier, and another portion is lost when the fluid enters the vortex valve chamber. If the pressure recoverable in the output leg of the amplifier is  $R_1(P_o - P_i)$ , where  $R_1$  is an assumed pressure recovery factor, then the total pressure recovered in the vortex valve is  $P_i + R_1 R_2 (P_o - P_i)$ , where  $R_2$  is the fraction of the remaining kinetic energy recovered in the vortex valve. The flow rate through the vortex valve is thus

$$Q = A_2 k_2 \sqrt{2 \left[ P_i + R_1 R_2 (P_o - P_i) - P_B \right] / \rho} \quad , \quad (3)$$

where  $A_2$  is the area of the vortex valve outlet,  $k_2$  is the associated discharge coefficient, and  $P_B$  is the back pressure on the vortex valve. Equation (2) may be used to eliminate  $P_i$  so that

$$Q = A_2 k_2 \sqrt{2 \left[ P_o - P_B - \left( 1 - R_1 R_2 \right) \frac{\rho}{2} \left( \frac{v_{pj}}{k_1} \right)^2 \right] / \rho} \quad . \quad (4)$$

Equation (4) may be written completely in terms of measured parameters by use of equation (1). Solving for the vortex valve discharge coefficient,  $k_2$ , yields

$$k_2 = Q/A_2 \sqrt{2 \left[ (P_o - P_B)/\rho \right] - \left( 1 - R_1 R_2 \right) Q^2 / A_1^2 K_1^2} \quad . \quad (5)$$

Equation (5) has been used in the analysis of experimental data taken on mud-pulser circuit A. The experiment and analysis are described in section 3.2.

The effective area,  $A_{eff}$ , of a pulser is defined as that area which, when subjected to the same pressure differential as the circuit, passes the same flow rate. The effective area is, thus, given by

$$A_{eff} = Q / \sqrt{2(P_o - P_B) / \rho} \quad (6)$$

Equation (6) can be used to calculate the effective area of a pulser circuit from experimentally determined values of flow rate and pressure drop.

By solving equation (5) for  $Q$  and combining it with equation (6), we can show that the effective area is given by

$$1/A_{eff}^2 = \left[ \left( 1 - R_1 R_2 \right) / A_{11}^2 k_1^2 \right] + 1/A_{22}^2 k_2^2 \quad (7)$$

Therefore, once discharge coefficients are known for the fluidic amplifier nozzle and the vortex valve exhaust nozzle, equation (7) may be used to estimate changes in a circuit's effective area as improvements are made in pressure recovery or discharge coefficient.

### 3. EXPERIMENTS AND RESULTS

#### 3.1 Introduction

An experimental investigation of pulser circuits A, B, and C has been conducted to (a) determine the performance changes in specific pulser test circuits when drilling muds are employed as the flow media, (b) relate changes in performance to changes in properties, (c) establish a method of estimating the type of performance which current circuit configurations would provide in a full-scale circulating system, and (d) estimate how possible design improvements might affect the overall functional characteristics of a fluidic mud-pulse telemetry transmitter.

The principal experiments were conducted on circuit A. These experiments consisted of measuring the pressure-flow characteristics of circuit A in the easy flow and restricted (hard) flow operating modes.

Additional experiments were conducted on circuits A, B, and C to verify amplifier bistability, to measure frequency response, and to provide qualitative information on flow modulation and overall performance.

The test circuits used in the experiments were formed in flat brass base plates by the use of an optical tracer milling machine. The base plate contained all flow channels. The channels were covered with a second plate which was secured with screws and contained pressure taps and control input connectors. Figure 5 shows the circuit A assembly.

The test fluids were formulated with water as the base fluid, bentonite to build viscosity, and barite as a weighting material. Table I lists properties of the three muds used to test the pulser (water was also used as a test fluid). Mud I was made from fresh water with 20 lb/barrel\* of bentonite. Mud I was an unweighted mud with a density of 8.4 ppg (pounds per gallon).† Mud II was made from Mud I by weighting it up with barite to a density of 12.0 ppg. Mud II was then diluted with water and weighted up with barite to a density of 15.3 ppg to make Mud III. Mud rheological properties were measured with a Baroid variable-speed viscometer. The gel strength and yield point are considered quite high for Mud III, while its plastic viscosity and density have moderate to high values for drilling muds found in the field.

TABLE I. MUD PROPERTIES

Property	Mud I	Mud II	Mud III
Density (ppg) <sup>a</sup>	8.4	12	15.3
Plastic viscosity (cps) <sup>b</sup>	11	20	27
Yield point (lb/100 ft <sup>2</sup> ) <sup>c</sup>	8	19	6
Gel strength (lb/100 ft <sup>2</sup> )			
10 s	7	30	23
10 min	28	85	51

$$^a (\text{ppg}) 119.8 = (\text{kg}/\text{m}^3)$$

$$^b (\text{cps}) 10^{-3} = (\text{Pa} \cdot \text{s})$$

$$^c (\text{lb}/100 \text{ ft}^2) 0.4788 = (\text{Pa})$$

$$* (\text{lb}/\text{barrel}) = \sim (\text{g}/350 \text{ cm}^3).$$

$$^\dagger (\text{ppg}) 119.8 = (\text{kg}/\text{m}^3).$$

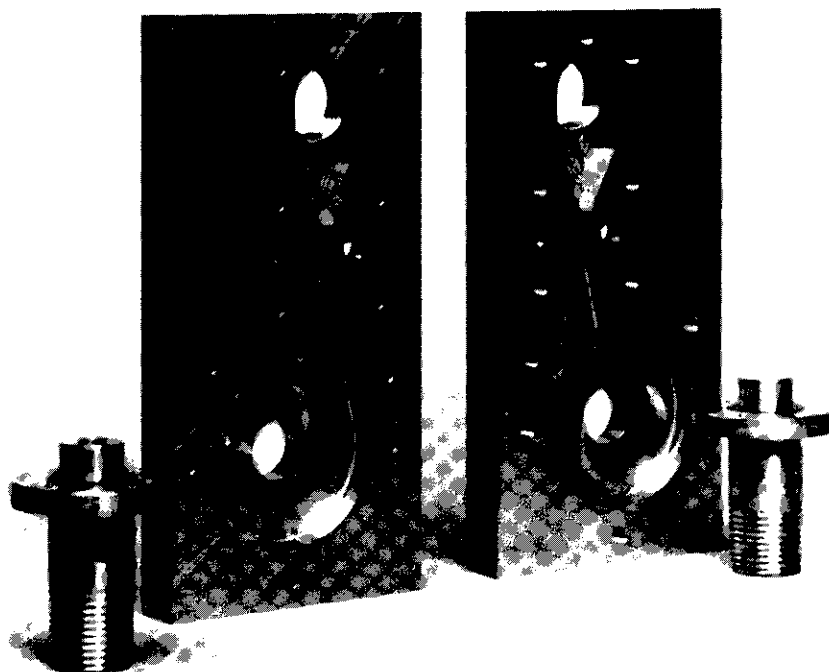


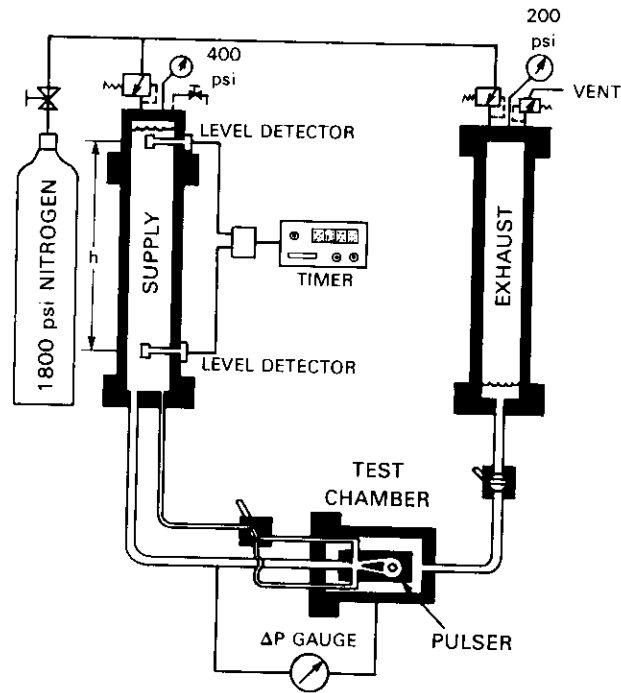
Figure 5. Circuit A assembly.

The test apparatus used for the circuit A experiments is shown schematically in figure 6. High-pressure nitrogen was used to circulate mud from the supply chamber through a second chamber containing the test circuit and into a reservoir chamber. The operating pressure across the test circuit was maintained by a supply regulator and a back-pressure regulator located on the top of each container.

A back pressure of 200 psi\* was maintained during all tests to eliminate cavitation in the circuit. This back pressure was considered high enough to eliminate cavitation for supply pressures up to 400 psi (200-psi differential pressure across the pulser). Higher back pressures were not considered necessary even though downhole well-bore pressures reach 10,000 psi or greater, because fluid properties (viscosity and density) do not change significantly even at these high pressures. Test fluid viscosities and densities varied over much wider ranges than back pressure can cause, so the tests are considered representative of downhole conditions.

---

\*(psi)6.895 = (kPa).



PULSER FLOW DIAGRAM

(psi) 6.895 = (kPa)

Figure 6. Test apparatus for circuit A.

The direction of flow through the test circuit (hard or easy flow state) was set during circulation but before flow measurements were made. The direction was set by allowing a pressurized flow to enter the required control port through a three-way valve. The control flow was then shut off while flow measurements were made.

The flow rate was determined from measurements of the time required to displace a known volume of fluid. Two ultrasonic level detectors located a fixed distance apart were used to actuate a timer. The distance between the detectors and the cross-sectional area of the chamber determined the supply volume, which was measured to be 3.01 gal.\*

---

\*(gal)  $3.785 \times 10^{-3} = (m^3)$ .

### 3.2 Test Results and Analysis--Circuit A

From equations (1) to (6) and from measured values of flow rate ( $Q$ ) versus pressure drop across the pulser ( $P_o - P_B$ ), it is possible to calculate jet velocities, internal static pressures ( $P_i$ ), and the discharge coefficient of the vortex valve--provided certain assumptions are made about dynamic losses in the pulser. In the following analysis of the data obtained on circuit A, it has been assumed that the pressure recovery ( $R_1$ ) of the fluidic amplifier is 0.5, a typical value for bistable amplifiers of this design. This assumption means that if the total pressure were measured in the output leg of the amplifier, it would be  $P_i + 0.5(P_o - P_i)$ . The jet from the output leg then enters the vortex valve. If it enters radially (the easy direction), then the vortex valve chamber acts like a pure volume and all the dynamic head is lost to turbulence. If it enters tangentially (the hard direction), then, ideally, all the energy in the jet forms the vortex, and none of the dynamic head is lost. Thus, in the following analysis of mud-pulser performance data, the pressure recovery ( $R_2$ ) of the vortex valve has been assumed to be zero in the easy direction and unity in the hard direction. The discharge coefficient of the fluid amplifier was assumed to be 0.95 in all calculations.

The most significant measure of pulser performance is its effective area,  $A_{eff}$ , defined in equation (6). It is this effective area that changes when the pulser switches between its easy and hard flow directions. The ratio (at a constant pressure drop across the pulser) of the effective area in the easy direction to the effective area in the hard direction is defined as the turndown ratio of the mud-pulser circuit.

The effective areas calculated from the data taken on pulser circuit A are presented in figure 7. This circuit had an amplifier power jet area of 0.04 in.<sup>2</sup>\* (0.4-in. depth, 0.1-in. width) and a vortex valve outlet area of 0.0556 in.<sup>2</sup> (0.266-in. diameter). Turndown ratios derived from these data are 2.7 for water, 2.45 for Mud I, and 2.35 for Muds II and III.

It is interesting to note that the effective area increases in both the easy and hard directions as the mud viscosity increases. In the easy direction, this increase is probably due to decreased turbulence in the vortex valve chamber; in the hard direction, the increase is probably due to increased radial leakage to the drain through the boundary layer of the vortex.

Maximum power jet velocities (neglecting losses) through the fluid amplifier are shown in figure 8 as a function of pressure drop across the pulser. These velocities were calculated from the data taken

---

\* (in.) 2.54 = (cm).

on the pulser and the dynamic head calculated from equations (1) and (2). These jet velocities are the highest velocities in the pulser and should be used for erosion considerations.

The vortex valve discharge coefficient (again calculated from data taken on the pulser) is shown in figure 9 as a function of pressure drop across the vortex valve. The coefficient in the easy direction varies from about 0.45 to 0.7. This low value indicates the possibility of some vorticity in the flow pattern in the vortex chamber even in the easy direction. Eliminating this vorticity could significantly improve the pulser performance--provided the fluidic amplifier could also be increased in size to keep the power jet velocities low. As shown in section 4, however, even the turndown ratios achieved with circuit A are sufficient for generating high-amplitude signal pressures in the mud flow. Further improvement of pulser efficiency, however, would allow greater design flexibility.

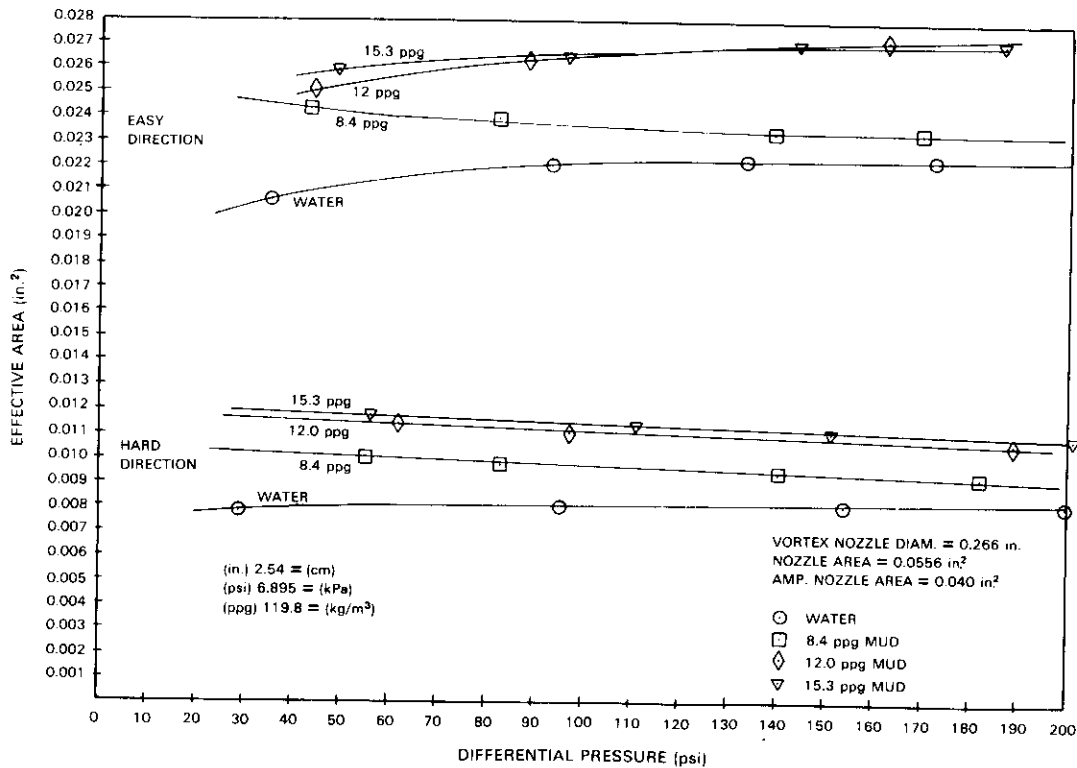


Figure 7. Effective area of circuit A versus pressure drop.

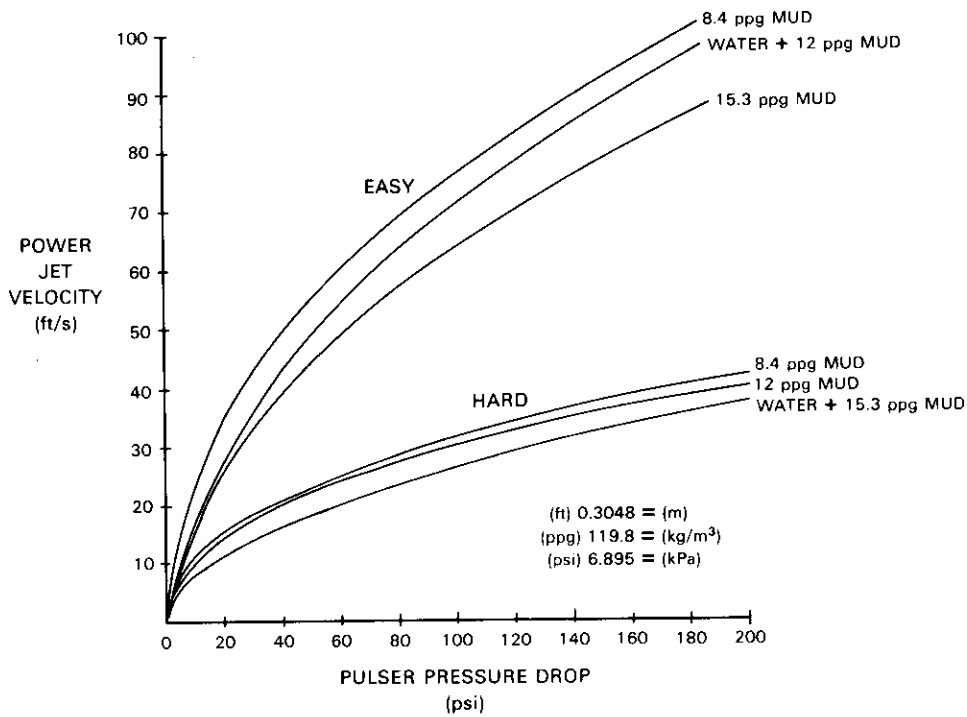


Figure 8. Power jet velocity for circuit A versus pressure drop.

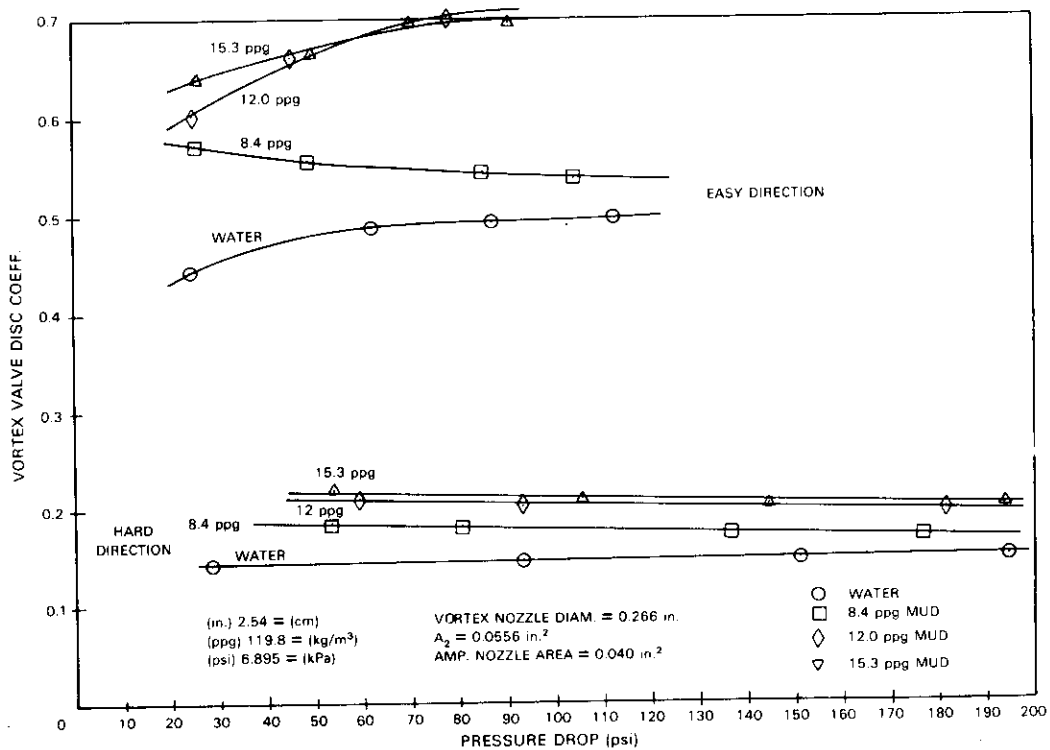


Figure 9. Vortex valve discharge coefficient versus pressure drop.



### 3.3 Mud-Pulser Flow Tests--Circuits B and C

The flow tests on circuit A showed that pulser performance could be significantly improved if the discharge coefficient of the vortex valve in the easy flow direction could be improved. Circuits B and C were designed to achieve this improvement.

In circuit B, the easy flow direction is not a stable state but exists only as the transition between the two states of high vorticity in opposite directions. Thus, the turndown ratio could not be directly measured. An experiment is currently under design to measure the turndown indirectly as a function of pressure drop across the pulser. Circuit B was operated with tap water at about 30-psi power jet pressure while high-speed movies were taken of the vortex valve exhaust flow. The movies showed that a jet of well-streamlined flow left the vortex valve between stable states of high vorticity. Figure 10 is a sample film strip. The sequential photographs illustrate the change in flow pattern at the exhaust nozzle of the pulser as it switches. The parallel streamlines indicate maximum flow from the pulser; the umbrella-shaped streamlines illustrate the high vorticity of the minimum flow condition.

In further tests on circuit B, the static pressure in the output leg of the fluidic amplifier was monitored with a piezoelectric pressure transducer. The pulser was supplied directly from a pressurized reservoir at pressures up to 60 psi. The supply pressure was thus constant during switching of the pulser; however, the static pressure in the output leg of the amplifier dropped significantly during switching because of the temporary increase in vortex valve effective area. It was not possible with the equipment used to obtain quantitative measurements of pressure amplitudes, but the duration of the pressure drop was determined. In this case the duration of the pressure drop indicates the period of the maximum operating frequency of the vortex valve.

The measurements showed that, for the subscale pulser tested, the period of switching is inversely proportional to flow rate (or the square root of the pressure drop) through the pulser. At 60-psi pressure drop across the pulser, the period was about 30 ms, corresponding to a frequency of 33 Hz. Tests with Mud III showed no difference in response time between mud and water.

Theory indicates that the response time of a vortex valve is inversely proportional to flow rate but directly proportional to the volume of the vortex chamber. This means that, when the present pulser is scaled up to a full-size operating valve, the response time will be proportional to the linear scaling factor. Present estimates are that a

full-scale (400 gal/min) pulser operating at a pressure differential of 100 psi or greater will have an upper cutoff frequency between 15 and 20 Hz. This should be considered a minimum estimate of cutoff frequency, because further improvements in valve dynamics can be expected.

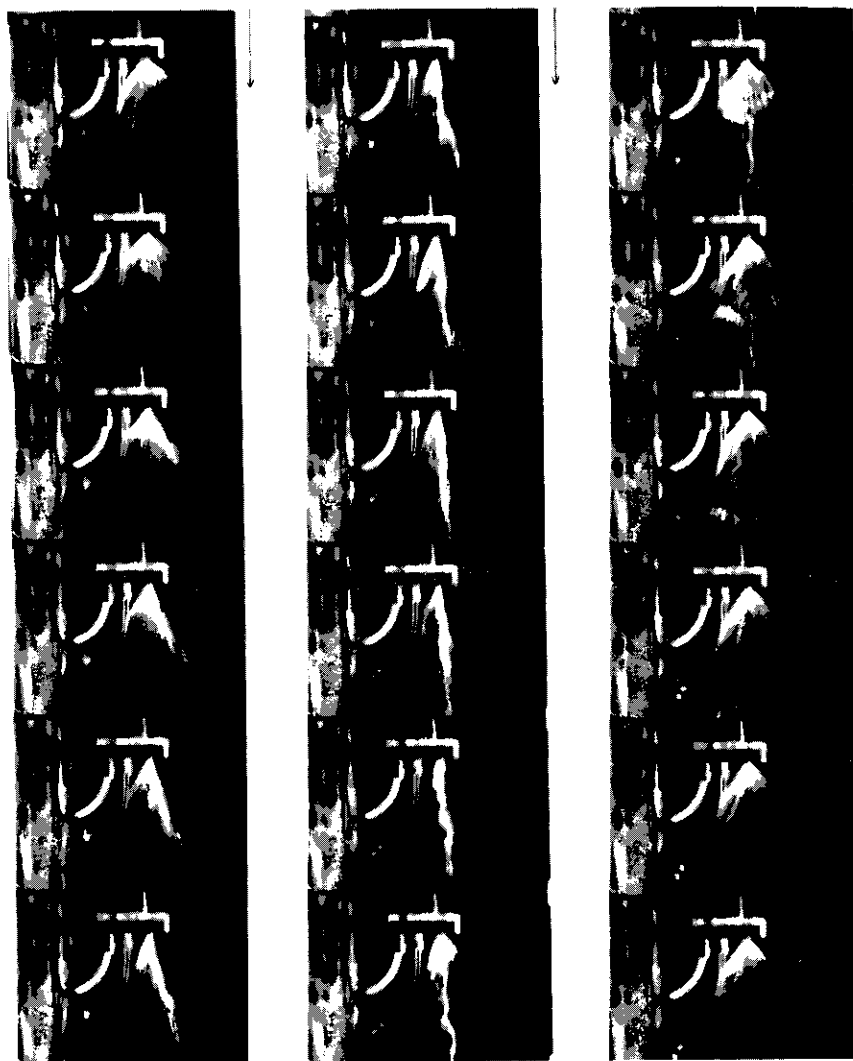


Figure 10. Sequential photographs of the switching of circuit B (200 frames/s).

Circuit C is a modification of circuit B to provide a stable easy flow condition. Only brief qualitative observations have been made to date on circuit C with tap water at low pressure differentials. These tests established that flows from the two inlets into the vortex valve could be balanced to provide a stable easy flow condition. Although no measurements were made, switching of the pulser appeared as rapid as for circuits A and B.

#### 4. ANALYSIS OF DYNAMIC PERFORMANCE IN A CIRCULATING SYSTEM

To predict the dynamic performance of a mud pulser in a circulating system, it is necessary to account for the dynamic flow conditions in the drill string as well as the performance of the pulser. If, for example, the pulser is close to the mud pump, the steady-state flow conditions will be attained quickly even if the effective area of the pulser is changed rapidly. Under steady flow conditions, the pressure drop across the valve will be inversely proportional to the square of the effective area of the pulser, because the flow rate will remain virtually constant even though the effective area of the valve has changed.

If, however, the pulser were situated downhole, a change in pressure at the pulser (caused by a change in pulser area) would not be sensed at the pump until the pulse traveled the distance between the pulser and pump at the speed of sound. Thus, by the time the mud pump is affected by the initial change in area, the pulser will have changed area many times. Under these conditions the flow rate through the pulser will not remain constant. For this case, the pressure signal generated by the pulser as its effective area is changed will be determined by the water-hammer relationship between the change in flow and the change in pressure.

The time-averaged flow rate through the pulser is determined by the pumping rate set at the surface. If the pulser is assumed to have two states with effective areas  $A_{1\text{eff}}$  and  $A_{2\text{eff}}$ , then there will be two flow rates,  $Q_1$  and  $Q_2$ , in the drill pipe at the pulser. If it is additionally assumed that the pulser spends equal times in these two states, then the average flow rate is  $(Q_1 + Q_2)/2$ . Thus, if the pump rate is  $Q$ , then

$$Q_1 + Q_2 = 2Q \quad . \quad (8)$$

The water-hammer relationship determines the relationship between the change in flow rate and the change in pressure upstream of the pulser; thus,

$$Q_1 - Q_2 = K(P_2 - P_1) \quad , \quad (9)$$

where  $K = A/\rho C$ ,  $A$  is the internal area of the pipe,  $\rho$  is the density of the fluid passing through the pulser,  $C$  is the speed of sound in the fluid, and  $P_1$  and  $P_2$  are the pressure upstream of the pulser for the two pulser states. If the pulser is assumed to be in series with and upstream of a drill bit with an effective area  $A_3$ , then the following equations relate the flow rate to the pressure drop across the pulser and the drill bit (pressure downstream of the drill bit is assumed constant and all pressures are referenced to it):

$$Q_1^2 = K_1^2 (P_1 - P_{B1}) \quad , \quad (10)$$

$$Q_1^2 = K_2^2 (P_2 - P_{B2}) \quad , \quad (11)$$

$$Q_1^2 = K_3^2 (P_{B1}) \quad , \quad (12)$$

$$Q_2^2 = K_3^2 (P_{B2}) \quad , \quad (13)$$

where, for the two pulser states,  $P_{B1}$  and  $P_{B2}$  are the pressures between the pulser and the bit,  $K_1 = A1_{\text{eff}} \sqrt{2/\rho}$ ,  $K_2 = A2_{\text{eff}} \sqrt{2/\rho}$ , and  $K_3 = A3 \sqrt{2/\rho}$ . These six equations--(8) through (13)--have six unknowns,  $Q_1$ ,  $Q_2$ ,  $P_1$ ,  $P_2$ ,  $P_{B1}$ , and  $P_{B2}$ , so they uniquely describe the operating conditions at the pulser when the pulser effective areas,  $A1_{\text{eff}}$  and  $A2_{\text{eff}}$ , the bit effective area,  $A_3$ , and the average flow rate,  $Q$ , are given.

Equations (8) through (13), when solved for  $Q_2$ , result in the following quadratic equation in  $Q_2$ .

$$Q_2^2 \left( \frac{1}{K_{23}^2} - \frac{1}{K_{13}^2} \right) + Q_2 \left( \frac{2}{K} + \frac{4Q}{K_{13}^2} \right) - \left( \frac{4Q^2}{K_{13}^2} + \frac{2Q}{K} \right) = 0 \quad , \quad (14)$$

where

$$1/K_{13}^2 = (1/K_1^2) + (1/K_3^2)$$

and

$$1/K_{23}^2 = (1/K_2^2) + (1/K_3^2)$$

If we define

$$a = \frac{1}{K_{23}^2} - \frac{1}{K_{13}^2},$$

$$b = \frac{2}{K} + \frac{4Q}{K_{13}^2}, \quad \text{and}$$

$$c = - \left( \frac{4Q}{K_{13}^2} \right) + \frac{2Q}{K}$$

then  $Q_2$  is given by

$$Q_2 = \frac{-b + \sqrt{b^2 - 4ac}}{2a} \quad (15)$$

From equations (8) through (13), the following relationships can be found.

$$Q_1 = 2Q - Q_2 \quad (16)$$

$$P_{B1} = Q_1^2/K_3^2 \quad (17)$$

$$P_{B2} = Q_2^2/K_{32}^2 \quad (18)$$

$$P_1 = Q_1^2/K_{13}^2 \quad (19)$$

$$P_2 = Q_2^2/K_{23}^2 \quad (20)$$

Thus, given the effective areas of the mud pulser ( $A_1$  and  $A_2$ ), the bit area ( $A_3$ ), the mud density ( $\rho$ ), and the average flow rate through the pulser (determined by the flow rate ( $Q$ ) at the pump), it is possible to calculate the dynamic downhole conditions. The results of such a calculation are shown in table II along with calculations of the steady-state pressure that would be expected if the pulser were closer to the mud pump or if it were steadily operated in either the easy or hard direction. The relationships in table II apply to any mud pulser in which the area changes are as indicated.

TABLE II. PULSER DYNAMIC PERFORMANCE

Drill pipe ID = 3.75 in. (9.52 cm)  
 Bit area = 0.35 in.<sup>2</sup> (2.26 cm<sup>2</sup>)  
 Mud density = 10 ppg (1198 kg/m<sup>3</sup>)  
 Sound speed = 4710 ft/s (1435 m/s)  
 Easy pulser area,  $A_{1eff} = 1.0$  in.<sup>2</sup> (6.45 cm<sup>2</sup>)

Average circulation flow rate (gal/min) <sup>a</sup>	Pulser operating conditions <sup>b</sup>										
	Steady state				Dynamic						
	Bit pressure (psi) <sup>c</sup>	Upstream pressure (psi) <sup>c</sup>		Signal pressure (psi) <sup>c</sup>	Flow rate (gal/min) <sup>a</sup>		Bit pressure (psi) <sup>c</sup>		Upstream pressure (psi) <sup>c</sup>		Signal pressure (psi) <sup>c</sup>
		Hard	Easy		Hard	Easy	Hard	Easy	Hard	Easy	
For flow rate = 100	75	108	83	25	97	103	70	79	102	88	14
200	299	432	332	100	192	208	275	324	397	360	37
400	1197	1728	1329	401	380	420	1078	1321	1557	1468	89
A <sub>2eff</sub> = 0.5 in. <sup>2</sup> (3.2 cm <sup>2</sup> ) (Turndown = 2)											
For flow rate = 100	75	208	83	125	88	112	57	94	159	105	54
200	299	831	332	499	168	232	211	402	587	447	140
400	1197	3322	1329	1993	325	475	792	1684	2200	1871	329
A <sub>2eff</sub> = 0.25 in. <sup>2</sup> (1.6 cm <sup>2</sup> ) (Turndown = 4)											

<sup>a</sup> (ft/s)0.3048 = (m/s)

<sup>b</sup> All pressures are referenced to downhole pressure

<sup>c</sup> (psi)6.895 = (kPa)

Examination of table II shows that the dynamic signal pressure (water hammer) is much less than would be expected from steady-state operating characteristics. However, if the turndown ratio is greater than 2 and the flow rate is 200 gal/min\* or higher, then the dynamic signal pressure is at least 37 psi.

Use of calculations such as these allows pulser size and turndown ratios to be optimized for a given bit area and mud flow rate. Accurate calculations of downhole conditions are also necessary for valid interpretation of field-test data.

$$*(\text{gal/min})6.31 \times 10^{-5} = \text{m}^3/\text{s}.$$

## 5. SUMMARY AND CONCLUSIONS

The HDL mud-pulser program is being conducted to determine areas in which fluidic technology can be applied for the improvement of mud-pulser valve speed and reliability. To date the program has consisted of an experimental and analytical study of three subscale fluidic mud-pulsing circuits. The results of the study are as follows.

(1) The unusual rheological properties of drilling mud do not significantly affect the bistable operation of digital fluidic amplifiers for the scale and flow rate of the tests.

(2) The increased viscosity of drilling mud causes a slight increase (relative to water) in the effective area of the vortex valve in both the maximum and minimum flow states.

(3) The turndown ratio of the experimental pulser circuit A varied from 2.7 for water to 2.35 for 15.3 ppg mud.

(4) The pulser turndown ratio can be improved over the experimental model by an increase in the vortex valve discharge coefficient in the maximum flow state.

(5) Measured response times for circuit B indicate that a full-scale pulser valve will have a frequency response of 15 to 20 Hz. This response could possibly be increased through improved valve dynamics.

(6) Calculations of dynamic conditions in the drill string indicate that the turndown ratios of the experimental pulser would generate signal pressures of at least 37 psi at a 200-gal/min circulation rate.

HDL is now engaged in an ongoing effort to optimize the geometry of the subscale pulser circuit for turndown ratio and frequency response. A full-scale pulser will then be constructed and tested under surface and downhole conditions so that predicted performance can be verified.





# NOMENCLATURE

$A$	Drill pipe internal area
$A_{eff}$	Effective areas of the mud-pulser valve, defined in equation (6)
$A_1$	Power jet area for the bistable amplifier
$A_{1eff}$	One of the two pulser effective areas
$A_2$	Area of the vortex valve outlet
$A_{2eff}$	One of the two pulser effective areas
$A_3$	Total bit nozzle effective area
$a$	Coefficient of quadratic equation
$b$	Coefficient of quadratic equation
$C$	Speed of sound
$c$	Coefficient of quadratic equation
$h$	Depth of vortex valve chamber
$K$	Water-hammer equation coefficient
$K_1$	Defined in text, equation (10)
$K_2$	Defined in text, equation (11)
$K_3$	Defined in text, equation (12)
$K_{13}$	Defined in text, equation (14)
$K_{23}$	Defined in text, equation (14)
$k_1$	Discharge coefficient for the bistable amplifier
$k_2$	Discharge coefficient for the vortex valve exhaust nozzle
$P_B$	Pressure downstream of the vortex valve
$P_{B1}$	One of the two drill-bit pressures during pulser operation (pulser effective area = $A_{1eff}$ )
$P_{B2}$	One of the two drill-bit pressures during pulser operation (pulser effective area = $A_{2eff}$ )

# NOMENCLATURE (Cont'd)

$P_i$	Internal static pressure in the bistable amplifier
$P_o$	Total pressure supplied to the mud pulser
$P_1$	One of the two pressures upstream of the pulser during operation (pulser effective area = $A_{1_{eff}}$ )
$P_2$	One of the two pressures upstream of the pulser during operation (pulser effective area = $A_{2_{eff}}$ )
$Q$	Average flow rate through the pulser
$Q_1$	One of the two flow rates through the pulser during operation (pulser effective area = $A_{1_{eff}}$ )
$Q_2$	One of the two flow rates through the pulser during operation (pulser effective area = $A_{2_{eff}}$ )
$R_1$	Pressure recovery of the bistable amplifier
$R_2$	Pressure recovery in the vortex valve
$r_e$	Vortex valve exhaust nozzle radius
$r_o$	Vortex valve chamber radius
$v_{pj}$	Bistable amplifier power jet velocity
$\rho$	Fluid density

# DISTRIBUTION

COMMANDER IDDR&E  
PENTAGON, ROOM 3D 1089  
WASHINGTON, DC 20310  
ATTN LTC G. KOPESAK

DEFENSE DOCUMENTATION CENTER  
CAMERON STATION, BUILDING 5  
ALEXANDRIA, VA 22314  
ATTN DDC-TCA (12 COPIES)

COMMANDER  
US ARMY RSCH & STD GP (EUR)  
ATTN LTC JAMES M. KENNEDY, JR.  
CHIEF, PHYSICS & MATH BRANCH  
EPO NEW YORK 09510

COMMANDER  
US ARMY MATERIEL DEVELOPMENT &  
READINESS COMMAND  
ATTN DRXAM-TL, HQ TECH LIBRARY  
5001 EISENHOWER AVENUE  
ALEXANDRIA, VA 22333

COMMANDER  
US ARMY MISSILE & MUNITIONS  
CENTER & SCHOOL  
ATTN ATSK-CTD-F  
REDSTONE ARSENAL, AL 35809

DIRECTOR  
US ARMY MATERIEL SYSTEMS  
ANALYSIS ACTIVITY  
ATTN DRXSY-MP  
ABERDEEN PROVING GROUND, MD 21005

DIRECTOR  
US ARMY BALLISTIC RESEARCH LABORATORY  
ATTN DRDAR-TSB-S (STINFO)  
ABERDEEN PROVING GROUND, MD 21005

TELEDYNE BROWN ENGINEERING  
CUMMINGS RESEARCH PARK  
ATTN DR. MELVIN L. PRICE, MS-44  
HUNTSVILLE, AL 35807

CONSERVATION DIVISION  
US GEOLOGICAL SURVEY  
12201 SUNRISE VALLEY DRIVE  
RESTON, VA 22070  
ATTN JOHN GREGORY (50 COPIES)

OFFICE OF THE DEPUTY CHIEF OF STAFF  
FOR RESEARCH, DEVELOPMENT &  
ACQUISITION  
DEPARTMENT OF THE ARMY  
WASHINGTON, DC 20310  
ATTN DAMA-ARP-P, DR. V. GARBER  
ATTN MR. JOHN HILL, ROOM 3D424

US ARMY R&D GROUP (EUROPE)  
BOX 15  
FPO NEW YORK 09510  
ATTN CHIEF, AERONAUTICS BRANCH  
ATTN CHIEF, ENGINEERING SCIENCES

US ARMY RESEARCH OFFICE  
P. O. BOX 12211  
RESEARCH TRIANGLE PARK, NC 27709  
ATTN JAMES J. MURRAY, ENG SCI DIV

BMD ADVANCED TECHNOLOGY CENTER  
P.O. BOX 1500  
HUNTSVILLE, AL 35807  
ATTN J. PAPADOPOULOS

COMMANDER  
USA FOREIGN SCIENCE & TECHNOLOGY CENTER  
FEDERAL OFFICE BUILDING  
220 7th STREET, NE  
CHARLOTTEVILLE, VA 22901  
ATTN DRXST-SD1

DIRECTOR  
APPLIED TECHNOLOGY LABORATORY  
FORT EUSTIS, VA 23604  
ATTN GEORGE W. FOSDICK, DAVDL-EU-SYA

COMMANDER  
USA MISSILE RES & DEV COMMAND  
REDSTONE ARSENAL, AL 35809  
ATTN REDSTONE SCIENTIFIC INFORMATION  
CENTER, DRSMI-RBD  
ATTN DRDMI-TGC, WILLIAM GRIFFITH  
ATTN DRDMI-TGC, J. C. DUNAWAY  
ATTN DRCPM-TOE, FRED J. CHEPLEN

COMMANDER  
USA MOBILITY EQUIPMENT R&D CENTER  
FORT BELVOIR, VA 22060  
ATTN TECHNICAL LIBRARY (VAULT)  
ATTN DRDME-EM, R. N. WARE

COMMANDER  
EDGEWOOD ARSENAL  
ABERDEEN PROVING GROUND, MD 21010  
ATTN SAREA-MT-T, MR. D. PATTON

COMMANDER  
US ARMY ARRADCOM  
DOVER, NJ 07801  
ATTN SARPA-TS-S-#59  
ATTN DRDAR-LCN-F, A. E. SCHMIDLIN  
ATTN DRDAR-LCW-E, MR. J. CONNOR

COMMANDER  
WATERVLIET ARSENAL  
WATERVLIET ARSENAL, NY 12189  
ATTN SARWV-RDT-L

DISTRIBUTION (Cont'd)

COMMANDER  
USA TANK AUTOMOTIVE RES & DEV COMMAND  
ARMOR & COMP DIV, DDDTA-RKT  
BLDG 215  
WARREN, MI 48090  
ATTN T. KOZOWYK  
ATTN M. STEELE

COMMANDER  
WHITE SANDS MISSILE RANGE, NM 88002  
ATTN STEWS-AD-L, TECHNICAL LIBRARY

COMMANDER  
US ARMY ARMAMENT MATERIEL  
READINESS COMMAND  
ROCK ISLAND, IL  
ATTN DRSAR-RDG-T, MR. R. SPENCER  
ATTN DRSAR-ASF  
ATTN DRSAR-LEP-L, TECHNICAL LIBRARY

COMMANDER/DIRECTOR  
ATMOSPHERIC SCIENCES LABORATORY  
USA ERADCOM  
WHITE SANDS MISSILE RANGE, NM 88002  
ATTN DELAS-AS (HOLT)

OFFICE OF NAVAL RESEARCH  
DEPARTMENT OF THE NAVY  
ARLINGTON, VA 22217  
ATTN STANLEY W. DOROFF, CODE 438  
ATTN D. S. SERGEL, CODE 211

DEPARTMENT OF THE NAVY  
R&D PLANS DIVISION  
ROOM 5D760, PENTAGON  
WASHINGTON, DC 20350  
ATTN BENJ R. PETRIE, JR.  
OP-987P4

COMMANDER  
NAVAL AIR DEVELOPMENT CENTER  
WARMINSTER, PA 18974  
ATTN R. MCGIBONEY, 30424  
ATTN CODE 8134, LOIS GUISE

NAVAL AIR SYSTEMS COMMAND  
DEPARTMENT OF THE NAVY  
WASHINGTON, DC 20360  
ATTN CODE AIR-52022A, J. BURNS  
ATTN CODE AIR-52022E, D. HOUCK

COMMANDER  
PACIFIC MISSILE RANGE  
NAVAL MISSILE CENTER  
POINT MUGU, CA 93042  
ATTN CODE 3123, ABE J. GARRETT  
ATTN CODE 1243, A. ANDERSON

COMMANDER  
NAVAL SHIP ENGINEERING CENTER  
PHILADELPHIA DIVISION  
PHILADELPHIA, PA 19112  
ATTN CODE 6772, D. KEYSER

COMMANDER  
NAVAL SURFACE WEAPONS CENTER  
WHITE OAK, MD 20910  
ATTN CODE 413, CLAYTON MCKINDRA  
ATTN CODE WA-33, J. O'STEEN

COMMANDER  
NAVAL ORDNANCE STATION  
INDIANHEAD, MD 20640  
ATTN CODE 5123B, J. MORRIS

NAVAL SHIP RES & DEV CENTER  
CODE 1619, MR. K. READER  
BETHESDA, MD 20084

NAVAL SEA SYSTEMS COMMAND  
SEA0331H  
WASHINGTON, DC 20362  
ATTN A. CHAIKIN

COMMANDER  
NAVAL WEAPONS CENTER  
CHINA LAKE, CA 93555  
ATTN CODE 533, LIBRARY DIVISION  
ATTN CODE 5536, MR. M. D. JACOBSON

COMMANDER  
AF AERO PROPULSION LABORATORY, AFSC  
WRIGHT-PATTERSON AFB, OH 45433  
ATTN LESTER SMALL 1TBC

COMMANDER  
AIR FORCE AVIONICS LABORATORY  
WRIGHT-PATTERSON AFB, OH 45433  
ATTN RWN-2, RICHARD JACOBS

DIRECTOR  
AF OFFICE OF SCIENTIFIC RESEARCH  
1400 WILSON BLVD  
ARLINGTON, VA 22209  
ATTN NE, MR. GEORGE KNAUSENBERGER

COMMANDER  
AIR FORCE FLIGHT DYNAMICS LABORATORY  
WRIGHT-PATTERSON AFB, OH 45433  
ATTN AFFDL/FGL, H. SNOWBALL

COMMANDER  
AF WEAPONS LABORATORY, AFSC  
KIRTLAND AFB, NM 87117  
ATTN SUL, TECHNICAL LIBRARY

DISTRIBUTION (Cont'd)

COMMANDER ARMAMENT DEVELOPMENT AND TEST CENTER EGLIN AIR FORCE BASE, FL 32542 ATTN ADTC (DLOSL), TECH LIBRARY	DEPARTMENT OF COMMERCE NATIONAL BUREAU OF STANDARDS WASHINGTON, DC 20234 ATTN GUSTAVE SHAPIRO, 425.00
AIR FORCE FLIGHT TEST CENTER 6510 ABG/SSD EDWARDS AFB, CA 93523 ATTN TECHNICAL LIBRARY	NASA AMES RESEARCH CENTER MOFFETT FIELD, CA 94035 ATTN MS 244-13, DEAN CHISEL
AF INSTITUTE OF TECHNOLOGY, AU WRIGHT-PATTERSON AFB, OH 45433 ATTN LIBRARY AFIT(LD), BLDG 640, AREA B ATTN AFIT(ENM), MILTON E. FRANKE	NASA LANGLEY RESEARCH CENTER HAMPTON, VA 23665 ATTN MS 494, H. D. GARNER ATTN MS 494, R. R. HELLBAUM ATTN MS 185, TECHNICAL LIBRARY
AEROSPACE MEDICAL DIVISION BROOKS AFB, TX 78235 ATTN AMD/RDN, CPT G. JAMES	NASA LEWIS RESEARCH CENTER 21000 BROOKPARK ROAD CLEVELAND, OH 44135 ATTN VERNON D. GEBBEN
DIV. OF REACTOR RES & DEV F-309 USERDA WASHINGTON, DC 20545 ATTN FRANK C. LEGLER	NASA SCIENTIFIC & TECH INFO FACILITY P. O. BOX 8657 BALTIMORE/WASHINGTON INTERNATIONAL AIRPORT, MD 21240 ATTN ACQUISITIONS BRANCH
OAK RIDGE NATIONAL LABORATORY CENTRAL RES LIBRARY, BLDG 4500N, RM 175 P. O. BOX X OAK RIDGE, TN 37830 ATTN E. HOWARD	UNIVERSITY OF ALABAMA CIVIL & MINERAL ENGINEERING DEPT. P. O. BOX 1468 UNIVERSITY, AL 35486 ATTN DR. HAROLD R. HENRY
DEPT OF HEW PUBLIC HEALTH SERVICE NATIONAL INSTITUTE OF HEALTH BLDG 13, RM 3W-13 BETHESDA, MD 20014 ATTN C. J. MCCARTHY	ARIZONA STATE UNIVERSITY ENGINEERING CENTER TEMPE, AZ 85281 ATTN PETER K. STEIN, LABORATORY FOR MEASUREMENT SYSTEMS ENGR.
DEPARTMENT OF COMMERCE NATIONAL BUREAU OF STANDARDS WASHINGTON, DC 20234 ATTN DR. JAMES SCHOOLEY, CHIEF, TEMPERATURE SECTION ATTN DR. T. NEGAS, MATERIALS DIVISION	UNIVERSITY OF ARKANSAS TECHNOLOGY CAMPUS P. O. BOX 3017 LITTLE ROCK, AR 72203 ATTN PAUL C. MCLEOD
DEPARTMENT OF COMMERCE BUREAU OF EAST-WEST TRADE OFFICE OF EXPORT ADMINISTRATION WASHINGTON, DC 20230 ATTN WALTER J. RUSNACK	UNIVERSITY OF ARKANSAS MECHANICAL ENGINEERING FAYETTEVILLE, AR 72701 ATTN JACK H. COLE, ASSOC PROF
SCIENTIFIC LIBRARY US PATENT OFFICE WASHINGTON, DC 20231 ATTN MRS. CURETON	CARNEGIE-MELLON UNIVERSITY SCHENLEY PARK PITTSBURGH, PA 15213 ATTN PROF W. T. ROULEAU, MECH ENGR DEPT
	CASE WESTERN RESERVE UNIVERSITY UNIVERSITY CIRCLE CLEVELAND, OH 44106 ATTN PROF P. A. ORNER

DISTRIBUTION (Cont'd)

THE CITY COLLEGE OF THE CITY  
UNIVERSITY OF NY  
DEPT OF MECH ENGR  
139th ST. AT CONVENT AVE  
NEW YORK, NY 10031  
ATTN PROF L. JIJI  
ATTN PROF G. LOWEN

DUKE UNIVERSITY  
COLLEGE OF ENGINEERING  
DURHAM, NC 27706  
ATTN C. M. HARMAN

ENGINEERING SOCIETIES LIBRARY  
345 EAST 47TH STREET  
NEW YORK, NY 10017  
ATTN HOWARD GORDON  
ATTN ACQUISITIONS DEPARTMENT

FRANKLIN INSTITUTE OF THE STATE  
OF PENNSYLVANIA  
20TH STREET & PARKWAY  
PHILADELPHIA, PA 19103  
ATTN KA-CHEUNG TSUI, ELEC ENGR DIV  
ATTN C. A. BELSTERLING

HUGHES HELICOPTERS  
DIVISION OF SUMMA CORPORATION  
CENTINELA & TEALE STREETS  
CULVER CITY, CA 90230  
ATTN LIBRARY 2/T2124

IIT RESEARCH INSTITUTE  
10 WEST 35th STREET  
CHICAGO, IL 60616  
ATTN DR. K. E. MCKEE

JOHNS HOPKINS UNIVERSITY  
APPLIED PHYSICS LABORATORIES  
LAUREL, MD 20810  
ATTN MR. MAYNARD HILL  
ATTN MR. THOMAS RANKIN  
ATTN MR. JOSEPH WALL

LEHIGH UNIVERSITY  
DEPARTMENT OF MECHANICAL ENGINEERING  
BETHLEHEM, PA 18015  
ATTN PROF FORBES T. BROWN

LINDA HALL LIBRARY  
5109 CHERRY STREET  
KANSAS CITY, MO 64110  
ATTN DOCUMENTS DIVISION

MASSACHUSETTS INSTITUTE OF TECHNOLOGY  
77 MASSACHUSETTS AVENUE  
CAMBRIDGE, MA 02139  
ATTN ENGINEERING TECHNICAL REPORTS,  
RM 10-408  
ATTN DAVID WORMLEY, MECH ENGR DEPT,  
RM 3-146

MICHIGAN TECHNOLOGICAL UNIVERSITY  
LIBRARY, DOCUMENTS DIVISION  
HOUGHTON, MI 49931  
ATTN J. HAWTHORNE

UNIVERSITY OF MISSISSIPPI  
201 CARRIER HALL, DEPT OF MECH ENGR  
UNIVERSITY, MS 38677  
ATTN DR. JOHN A. FOX

MISSISSIPPI STATE UNIVERSITY  
DRAWER ME  
STATE COLLEGE, MS 39672  
ATTN DR. C. J. BELL, MECH ENG DEPT

UNIVERSITY OF NEBRASKA LIBRARIES  
ACQUISITIONS DEPT, SERIALS SECTION  
LINCOLN, NE 68508  
ATTN ALAN GOULD

UNIVERSITY OF NEW HAMPSHIRE  
MECH ENGR DEPT, KINGSBURY HALL  
DURHAM, NH 03824  
ATTN PROF CHARLES TATE

DEPARTMENT OF MECHANICAL ENGINEERING  
NEWARK COLLEGE OF ENGINEERING  
323 HIGH STREET  
NEWARK, NJ 07102  
ATTN DR. R. Y. CHEN

OHIO STATE UNIVERSITY LIBRARIES  
SERIAL DIVISION, MAIN LIBRARY  
1858 NEIL AVENUE  
COLUMBUS, OH 43210

OKLAHOMA STATE UNIVERSITY  
SCHOOL OF MECH & AEROSPACE ENGR.  
STILLWATER, OK 74074  
ATTN PROF KARL N. REID

MIAMI UNIVERSITY  
DEPT OF ENG TECH  
SCHOOL OF APPLIED SCIENCE  
OXFORD, OH 45056  
ATTN PROF S. B. FRIEDMAN

PENNSYLVANIA STATE UNIVERSITY  
215 MECHANICAL ENGINEERING BUILDING  
UNIVERSITY PARK, PA 16802  
ATTN DR. J. L. SHEARER

PENNSYLVANIA STATE UNIVERSITY  
ENGINEERING LIBRARY  
201 HAMMOND BLDG  
UNIVERSITY PARK, PA 16802  
ATTN M. BENNETT, ENGINEERING LIBRARIAN

DISTRIBUTION (Cont'd)

PURDUE UNIVERSITY  
SCHOOL OF MECHANICAL ENGINEERING  
LAFAYETTE, IN 47907  
ATTN PROF. VICTOR W. GOLDSCHMIDT  
ATTN PROF. ALAN T. McDONALD

ROCK VALLEY COLLEGE  
3301 NORTH MULFORD ROAD  
ROCKFORD, IL 61101  
ATTN KEN BARTON

RUTGERS UNIVERSITY  
LIBRARY OF SCIENCE & MEDICINE  
NEW BRUNSWICK, NJ 08903  
ATTN GOVERNMENT DOCUMENTS DEPT  
MS. SANDRA R. LIVINGSTON

SYRACUSE UNIVERSITY  
DEPT OF MECH & AEROSPACE ENGINEERING  
139 E. A. LINK HALL  
SYRACUSE, NY 13210  
ATTN PROFESSOR D. S. DOSANJH

UNIVERSITY OF TEXAS AT AUSTIN  
DEPT OF MECHANICAL ENGINEERING  
AUSTIN, TX 78712  
ATTN DR. A. J. HEALEY

THE UNIVERSITY OF TEXAS AT ARLINGTON  
MECHANICAL ENGINEERING DEPARTMENT  
ARLINGTON, TX 76019  
ATTN DR. ROBERT L. WOODS

TULANE UNIVERSITY  
DEPT OF MECHANICAL ENGINEERING  
NEW ORLEANS, LA 70118  
ATTN H. F. HRUBECKY

UNION COLLEGE  
MECHANICAL ENGINEERING  
SCHENECTADY, NY 12308  
ATTN ASSOC PROF W. C. AUBREY  
MECH ENGR DEPT, STEINMETZ HALL

VIRGINIA POLYTECHNIC INSTITUTE OF STATE UNIV  
MECHANICAL ENGINEERING DEPARTMENT  
BLACKSBURG, VA 24061  
ATTN PROF H. MOSES

WASHINGTON UNIVERSITY  
SCHOOL OF ENGINEERING  
P. O. BOX 1185  
ST. LOUIS, MO 63130  
ATTN W. M. SWANSON

WEST VIRGINIA UNIVERSITY  
MECHANICAL ENGINEERING DEPARTMENT  
MORGANTOWN, WV 26505  
ATTN DR. RICHARD A. BAJURA

WICHITA STATE UNIVERSITY  
WICHITA, KS 67208  
ATTN DEPT AERO ENGR, E. J. RODGERS

UNIVERSITY OF WISCONSIN  
MECHANICAL ENGINEERING DEPARTMENT  
1513 UNIVERSITY AVENUE  
MADISON, WI 53706  
ATTN FEDERAL REPORTS CENTER  
ATTN NORMAN H. BEACHLEY, DIR,  
DESIGN ENGINEERING LABORATORIES

WORCESTER POLYTECHNIC INSTITUTE  
WORCESTER, MA 01609  
ATTN GEORGE C. GORDON LIBRARY (TR)  
ATTN TECHNICAL REPORTS

AIRESEARCH  
P. O. BOX 5217  
402 SOUTH 36th STREET  
PHOENIX, AZ 85034  
ATTN DAVID SCHAFFER  
ATTN TREVOR SUTTON  
ATTN TOM TIPPETTS

AVCO SYSTEMS DIVISION  
201 LOWELL STREET  
WILMINGTON, MA 01887  
ATTN W. K. CLARK

BELL HELICOPTER COMPANY  
P. O. BOX 482  
FORTWORTH, TX 76101  
ATTN MR. R. D. YEARY

BENDIX CORPORATION  
ELECTRODYNAMICS DIVISION  
11600 SHERMAN WAY  
N. HOLLYWOOD, CA 90605  
ATTN MR. D. COOPER

BENDIX CORPORATION  
RESEARCH LABORATORIES DIV.  
BENDIX CENTER  
SOUTHFIELD, MI 48075  
ATTN C. J. AHERN

BOEING COMPANY, THE  
P. O. BOX 3707  
SEATTLE, WA 98124  
ATTN HENRIK STRAUB

BOWLES FLUIDICS CORPORATION  
9347 FRASER AVENUE  
SILVER SPRING, MD 20910  
ATTN VICE PRES./ENGR.

DR. RONALD BOWLES  
2105 SONDRAL COURT  
SILVER SPRING, MD 20904

DISTRIBUTION (Cont'd)

CONTINENTAL CAN COMPANY  
TECH CENTER  
1350 W. 76TH STREET  
CHICAGO, IL 60620  
ATTN P. A. BAUER

CORDIS CORPORATION  
P. O. BOX 428  
MIAMI, FL 33137  
ATTN STEPHEN F. VADAS, K-2

CORNING GLASS WORKS  
FLUIDIC PRODUCTS  
HOUGHTON PARK, B-2  
CORNING, NY 14830  
ATTN MR. W. SCHEMERHORN

CHRYSLER CORPORATION  
P.O. BOX 118  
CIMS-418-33-22  
DETROIT, MI 48231  
ATTN MR. L. GAU

EMX ENGINEERING, INC  
BOX 216 - 216 LITTLE FALLS RD  
CEDAR GROVE, NJ 07009  
ATTN ANTHONY P. CORRADO, PRESIDENT

FLUIDICS QUARTERLY  
P. O. BOX 2989  
STANFORD, CA 94305  
ATTN D. H. TARUMOTO

GENERAL ELECTRIC COMPANY  
SPACE/RESD DIVISIONS  
P. O. BOX 8555  
PHILADELPHIA, PA 19101  
ATTN MGR LIBRARIES, LARRY CHASEN

GENERAL MOTORS CORPORATION  
DELCO ELECTRONICS DIV  
MANFRED G. WRIGHT  
NEW COMMERCIAL PRODUCTS  
P. O. BOX 1104  
KOKOMO, IN 46901  
ATTN R. E. SPARKS

GRUMMAN AEROSPACE CORPORATION  
TECHNICAL INFORMATION CENTER  
SOUTH OYSTER BAY ROAD  
BETHPAGE, L. I., NY 11714  
ATTN C. W. TURNER, DOCUMENTS  
LIBRARIAN

HAMILTON STANDARD  
DIVISION OF UNITED AIRCRAFT  
CORPORATION  
WINDSOR LOCKS, CT 06096  
ATTN MR. PHILIP BARNES

HONEYWELL, INC.  
1625 ZARTHAN AVE  
MINNEAPOLIS, MI 55413  
ATTN J. HEDEEN

JOHNSON CONTROLS, INC  
507 E. MICHIGAN  
MILWAUKEE, WI 53201  
ATTN WARREN A. LEDERMAN

MOORE PRODUCTS COMPANY  
SPRING HOUSE, PA 19477  
ATTN MR. R. ADAMS

MARTIN MARIETTA CORPORATION  
AEROSPACE DIVISION  
P. O. BOX 5837  
ORLANDO, FL 32805  
ATTN R. K. BRODERSON, MP 326  
ATTN VITO O. BRAVO, MP 326

MCDONNELL AIRCRAFT COMPANY  
GUIDANCE AND CONTROL MECHANICS DIVISION  
ST. LOUIS, MO 63166  
ATTN MR. LOYAL GUENTHER

NATIONAL FLUID POWER ASSOCIATION  
3333 NORTH MAYFAIR ROAD  
MILWAUKEE, WI 53222  
ATTN JOHN R. LUEKE  
DIR OF TECH SERVICES

PLESSEY AEROSPACE LTD  
500 NORTHWEST PLAZA  
SUITE 814  
ST. ANN, MO 63074  
ATTN MR. GEORGE UPTON

RICHARD WHITE & ASSOCIATES  
ELECTRO/MECHANICAL ENGINEERS  
77 PELHAM ISLE ROAD  
SUDBURY, MA 01776  
ATTN RICHARD P. WHITE

ROCKWELL INTERNATIONAL CORPORATION  
COLUMBUS AIRCRAFT DIVISION, P. O. BOX 1259  
4300 E. 5TH AVENUE  
COLUMBUS, OH 43216  
ATTN MR. MARVIN SCHWEIGER

SANDIA CORPORATION  
KIRTLAND AFB, EAST  
ALBUQUERQUE, NM 87115  
ATTN WILLIAM R. LEUENBERGER, DIV 2323

TRITEC, INC  
P.O. BOX 56  
COLUMBIA, MD 21045  
ATTN L. SIERACKI



DISTRIBUTION (Cont'd)

UNITED TECHNOLOGIES RESEARCH CENTER  
400 MAIN STREET  
E. HARTFORD, CT 06108  
ATTN R. E. OLSON, MGR FLUID  
DYNAMICS LABORATORY

US ARMY ELECTRONICS RESEARCH  
& DEVELOPMENT COMMAND  
ATTN WISEMAN, ROBERT S., DR., DRDEL-CT

HARRY DIAMOND LABORATORIES  
ATTN 00100, COMMANDER/TECH DIR/TSO  
ATTN CHIEF, DIV 10000  
ATTN CHIEF, DIV 20000  
ATTN CHIEF, DIV 30000  
ATTN CHIEF, DIV 40000  
ATTN RECORD COPY, 81200  
ATTN HDL LIBRARY, 81100 (3 COPIES)  
ATTN HDL LIBRARY, 81100 (WOODBIDGE)  
ATTN TECHNICAL REPORTS BRANCH, 81300  
ATTN CHAIRMAN, EDITORIAL COMMITTEE  
ATTN COX, L. S. 00210  
ATTN EITNER, B. PAO  
ATTN CHIEF, 13000  
ATTN LANHAM, C 00210  
ATTN DRZEWIECKI, T. 13400  
ATTN GOTO, J. 13400  
ATTN HOLMES, A. 13400 (5 COPIES)  
ATTN GEHMAN, S. 13400 (5 COPIES)  
ATTN CHIEF, 13400 (10 COPIES)





